Effect of sodium trimetaphosphate modification on the structure and rheological properties of zein

Hao ZHANG[1], Yanyan ZHAO[1], Xiaofeng KANG[1], Hongbo LI[2], Haizhen MO[2]* (iD)

Abstract

The modification of zein with sodium trimetaphosphate (STMP) as a cross-linking agent was studied. The effects of the mass ratio of STMP to zein ($R_{S/Z}$), pH, reaction temperature and time on the rheological properties of modified zein solution (Z-SP) were evaluated. By using response surface methodology, the optimal modification conditions were also determined as following: $R_{S/Z}$ 0.03, pH 6.8, reaction time 2 h, reaction temperature 25 °C. Under these conditions, the observed shear stress of Z-SP solution was 35.0025 Pa, close to the predicted value. Compared with natural zein, the viscosity of Z-SP increased with the increasing shear rate, which was attributed to the structural changes, as evidenced by circular dichroism (CD) and Fourier transform infrared (FT-IR) analysis.

Keywords: zein; sodium trimetaphosphate; cross-linking; shear stress; circular dichroism.

Practical Application: This work systematically studied the modification of zein with sodium trimetaphosphate (STMP) as a cross-linking agent. This will provide a theoretical basis for preparing a cross-linked zein membrane and developing its application in foods.

1 Introduction

Zein, the main protein in corn, is rich in glutamic acid (21-26%), leucine (20%), proline (10%) and alanine (10%) (Kaya & Boccaccini, 2017). However, it lacks basic and acidic amino acids, especially tryptophan and lysine. It is a heterogeneous mixture of peptides with different molecular weights, solubility and charges connected by disulfide bonds. The average molecular weight is 4.4×10^4. Zein has good film-forming, gelling and antioxidant properties (Kasaai, 2018). But zein films have better brittleness and poor viscosity, extensibility and tensile strength, their mechanical properties cannot satisfy the actual production needs (Song & Wang, 2021; Zhang et al., 2015). Studies have shown that the brittleness and other mechanical properties of the film can be improved by adding a plasticizer and cross-linking agent (Cazón et al., 2017). However, the current cross-linking agents such as glutaraldehyde and epichlorohydrin have certain toxicity, which limits their application in food (Wang et al., 2018). STMP, with formula $Na_3P_3O_9$, is a metaphosphate of sodium, which is one of the safe, non-toxic cross-linking agents for starch approved by the Food and Drug Administration (Yıldırım-Yalçın et al., 2019). It can be used as a meat adhesive, dispersant, stabilizer, fruit juice turbidity prevention agent and starch modifier. In this study, STMP is used as a cross-linking agent to modify zein. This will provide a theoretical basis for preparing a cross-linked zein membrane and developing its application in foods.

2 Materials and methods

2.1 Materials

Zein and STMP (purity ≥ 95%) were purchased from Aladdin (Shanghai, China). Anhydrous ethanol, sodium hydroxide and hydrochloric acid were acquired from Sinopharm Chemical (Shanghai, China). The ultrapure water was from a Thermo Gen Pure UV/UF water system (Waltham, MA).

2.2 Methods

Modification of zein

Two grams of zein was dissolved in 100 mL of 80% ethanol solution to generate a 2% (m/V) zein solution. After a certain amount of STMP was added, they were incubated at the designed temperature for a specified time. The obtained mixture was dialyzed for 12 h with deionized water (Yıldırım-Yalçın et al., 2019; Khalil et al., 2015). The sediment was collected and freeze-dried as the modified zein (Z-SP).

Rheological measurement

The 80% ethanol solvent was used for preparing a 2% polymer (zein and Z-SP) solution for testing. The rheological measurement was carried out at a HAAKE MARS II rheometer (Thermo Fisher Scientific Co., Ltd, Waltham, MA, USA) with a cone-plate (C60/1°TiL) probe. The effect of shear rate (0.01 to 1000 s^{-1}) on the flowcurve were recording during 300 s (Bozdogan et al., 2022;

Nascimento et al., 2016). In the viscoelasticity (small amplitude oscillation shear) measurement, the frequency (f) scanning range was 0.1-100 Hz and the shear stress (τ) was 0.1 Pa (in the linear viscoelastic region). The test temperature was set at 25 ± 0.2 °C.

Optimization of the preparation process of Z-SP

According to the preparation method of Z-SP in section 2.2, the preparation process of Z-SP was optimized by using response surface methodology (Yao et al., 2022). When the reaction temperature was fixed at 25 °C, the experimental factors included the mass ratio of STMP to zein ($R_{S/Z}$), pH and reaction time. The corresponding factor levels were selected based on the central composite design (Table 1). The shear stress was used as the response value.

Fourier Transform Infrared (FT-IR) spectroscopy

The FT-IR spectra of zein and Z-SP were obtained on a Nico-let FT-IR 20 SX spectrometer (Nicolet, USA) based on the KBr method (Yan et al., 2022; Forato et al., 2003). The measurements were carried at 4 cm^{-1} resolution with 32 scans in the mid-infrared region (4000-400 cm^{-1}).

Circular Dichroism (CD) spectroscopy

The CD measurement was carried out on a Pistar π-180 CD spectropolarimeter (Applied Photo physics Ltd., UK). Both the spectra in the near ultraviolet range of 250-320 nm and the far ultraviolet range of 190-260 nm were recorded (Qi et al., 2015).

Statistical analysis

The assay was carried out based on three independent experiments. Statistical comparisons were performed using the *t*-test. A *p* value of < 0.05 was considered to be a significant difference.

3 Results and discussion

3.1 RSM model and ANOVA analysis

Response surface methodology (RSM) is a strong experimental tool, which can optimize the preparation process involving multiple factors. RSM usually fits a model based on the central composite design (CCD) by least squares technique. In this study, the experimental design and results are shown in Table 1. The shear stress ranged from 2.591 Pato 34.53 Pa. The maximum value was found at the $R_{S/Z}$ 0.03, pH 7.0 and the reaction time 2 h. By applying multiple regression analysis on the experimental data, the response variable and the test variables are related by the following second-order polynomial equation (Equation 1):

$$Shear\ stress = 23.30 + 24.55A - 0.66B + 2.43C - 1.46AB - 2.07AC + 0.95BC - 14.15A^2 - 9.77B^2 - 12.15C^2 \tag{1}$$

ANOVA and regression coefficients results of the quadratic model are shown in Table 2. The significance of quadratic regression model was tested by the value of F, *p* and correlation coefficient, and the corresponding results of ANOVA were exhibited in Table 2. It was found that all the *p* values of A, A^2, B^2 and C^2 were less than 0.05, which indicated that these variables were significant and had great influence on shear stress. The order of influence was as follows: $R_{S/Z}$ > pH > time. The F value was 1.52, and the *p* value was 0.3379. The *p* value was greater than 0.05, which suggested that the residual error of the model might be caused by random error. The value of determination coefficient (R^2 = 0.9611) indicated that the regression model was suitable for predicting shear stress. The correlation coefficient R^2 of the function was 0.9611, and the closer R^2 was to 1, the smaller the influence of error. The value of AdjR^2 (0.9377) was reasonably close to 1, demonstrating a high degree of correlation between the observed and predicted values. A very low value of coefficient of the variation (3.00%) clearly indicated a very high degree of precision and a good deal of reliability of the experimental.

3.2 Response surface analysis

The response surfaces of the regression model were obtained using SAS version 8.0 and are presented in Figure 1. The effect of $R_{S/Z}$ on the shear stress and its interaction with pH revealed that the shear stress increased with the increase of pH, and the shear stress was found to increase gradually with increase of pH from 5 to 7.7, but beyond 7.7, shear stress decreased with increasing pH. The effects of $R_{S/Z}$ and time on shear stress showed that the shear stress increased gradually with the increase of time when $R_{S/Z}$ was less than 0.03. And the effect of pH and time interaction on shear stress confirmed that the shear stress was the highest at neutral pH.

To verify the test results, the experimental rechecking was performed under the deduced optimal conditions ($R_{S/Z}$ 0.03, pH 6.8, reaction time 2 h and reaction temperature 25 °C). A mean value of 35.0025 pa (n = 3) was obtained, which was in agreement with the predicted value, demonstrating the validation of the model.

Table 1. Central composite design arrangement and response.

Treament	Independent variables			Shear stress (Pa)
	$R_{S/Z}$	pH	Time (h)	
Run	A	B	C	
1	0.03	7.0	2	34.530
2	0.03	9.0	2.5	10.042
3	0.03	7.0	2	32.206
4	0.03	7.0	2	31.721
5	0.03	7.0	2	32.037
6	0.03	5.0	2.5	10.901
7	0.04	5.0	2	11.222
8	0.02	5.0	2	14.061
9	0.03	7.0	2	38.037
10	0.02	7.0	1.5	7.909
11	0.03	9.0	1.5	10.754
12	0.04	7.0	2.5	2.755
13	0.04	7.0	1.5	2.854
14	0.04	9.0	2	2.591
15	0.02	7.0	2.5	16.107
16	0.03	5.0	1.5	15.422
17	0.02	9.0	2	11.278

Table 2. ANOVA analysis for the fitted model.

Source of variation	Sum of square	Degree of freedom	Mean square	F-value	P-value	Status
odel	2257.78	9	250.86	28.84	0.0001	Significant
A	112.00	1	112.00	12.88	0.0089	Significant
B	35.87	1	35.87	4.12	0.0818	Not significant
C	1.03	1	1.03	0.12	0.7412	Not significant
AB	8.55	1	8.55	0.98	0.3545	Not significant
AC	17.20	1	17.20	1.98	0.2024	Not significant
BC	3.63	1	3.63	0.42	0.5391	Not significant
A^2	842.58	1	842.58	96.88	< 0.0001	Significant
B^2	402.11	1	402.11	46.23	0.0003	Significant
C^2	621.97	1	621.97	71.51	< 0.0001	Significant
Residual	60.88	7	8.7			
Lack of fit	32.47	3	10.82	1.52	0.3379	Not significant
Pure error	28.41	4	7.10			
Cor total	2318.66	16				
Quadratic	**R^2**	**AdjR²**	**PredR²**	**C.V. %**	**PRESS**	**Adeq Precision**
summary statistics	0.9611	0.9377	0.8742	3.00	291.78	15.769
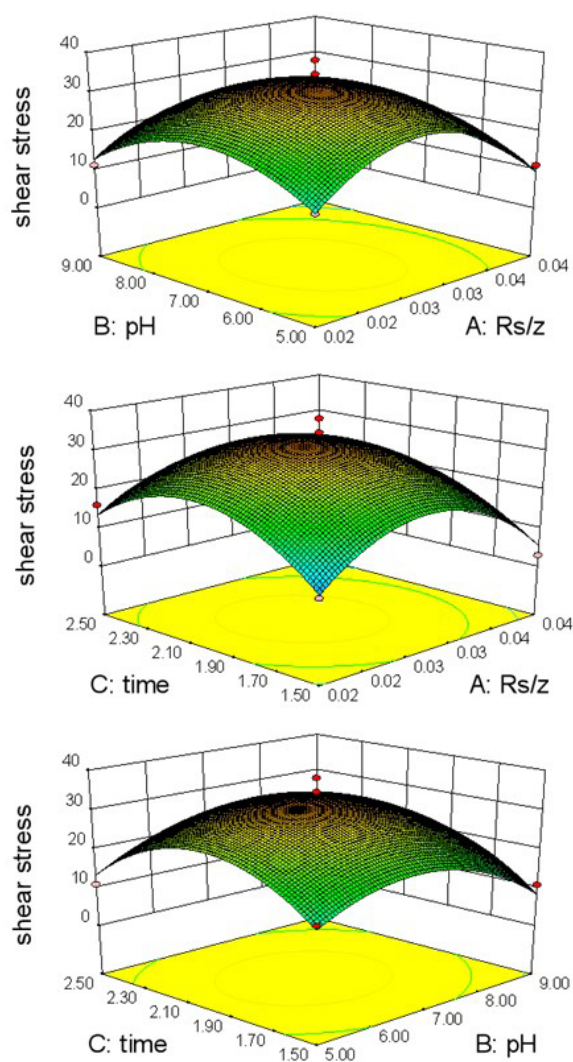
Figure 1. Response surfaces (3D) showing the effect of the $R_{S/Z}$, reaction time and pH on the shear stress.

3.3 Rheological analysis

Rheological analysis showed that the viscosities of Z-SP and zein gradually increased with the increase of shear rate (Figure 2). The viscosity of zein reduced with increasing pH. Because glutamic acid in protein is converted to glutamate with the increase of pH, which leads to the decomposition of zein aggregates in solution into monomer state and the decrease of viscosity (Zhang et al., 2011; Li et al., 2022). The viscosity of Z-SP was higher than that of zein. Z-SP had the highest viscosity at pH 7.0. Compared with zein, the high and low pH values had little effect on the viscosity of Z-SP.

3.4 CD analysis

Near ultraviolet CD is usually used to analyze the tertiary structure of proteins. Different aromatic ring amino acids have different absorptions within the range of 250-320 nm, and their peak type and intensity are determined by type, quantity, fluidity, microenvironment and spatial position of amino acids (Geng et al., 2022). In Figure 3, the near ultraviolet CD of zein had four peaks at 260, 270, 275 and 282 nm, which belonged to phenylalanine and tyrosine, respectively. There was no peak between 290 and 320 nm, which might be due to the low tryptophan content in zein molecules. It was observed that the near ultraviolet CD spectra of Z-SP and zein had only slight differences at different pH values (Figure 3A-3C). The peak shape was similar at pH 7.0 and 9.0, whereas the peak size at pH 5.0 was somewhat different, suggesting that zein had a similar tertiary structure in the three protein solutions (Figure 3D). After STMP phosphorylation in particular, the near-ultraviolet CD spectra of Z-SP with different pH values almost coincided, which meant that the cross-linking reaction between STMP and zein had no effect on the tertiary structure of the protein (Gouin, 2003).

Far ultraviolet CD can provide information on protein secondary structure. It could be observed that there was a positive peak near 195 nm and a strong negative peak near 205 and 225 nm, respectively (Figure 3E). When the pH of the protein
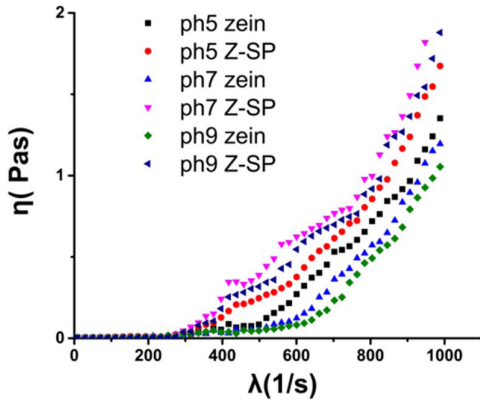
Figure 2. Changes in viscoelastic properties of Z-SP and zein with shear rate.

solution was 7.0, the negative peak intensity of the modified zein increased. When the pH of the protein solution was 5.0 or 9.0, the negative peak intensity of modified zein decreased (Byler & Susi, 1986; Greenfield, 2006).

The contents of α-helix, β-fold, β-turn and random curl in the protein were obtained by the DICHROWEB program (Figure 3F). Compared with zein, the α-helix and random coil contents of Z-SP decreased at pH 5.0 and 9.0. However, the β-fold content increased, indicating that the protein structure was more stable. At pH 7.0, the α-helix content increased while the β-folding and random curling contents decreased. After STMP was added, the α-helix and β-fold contents declined. However, the random coil content increased significantly, which meant that the protein structure was more prone to unfolding.
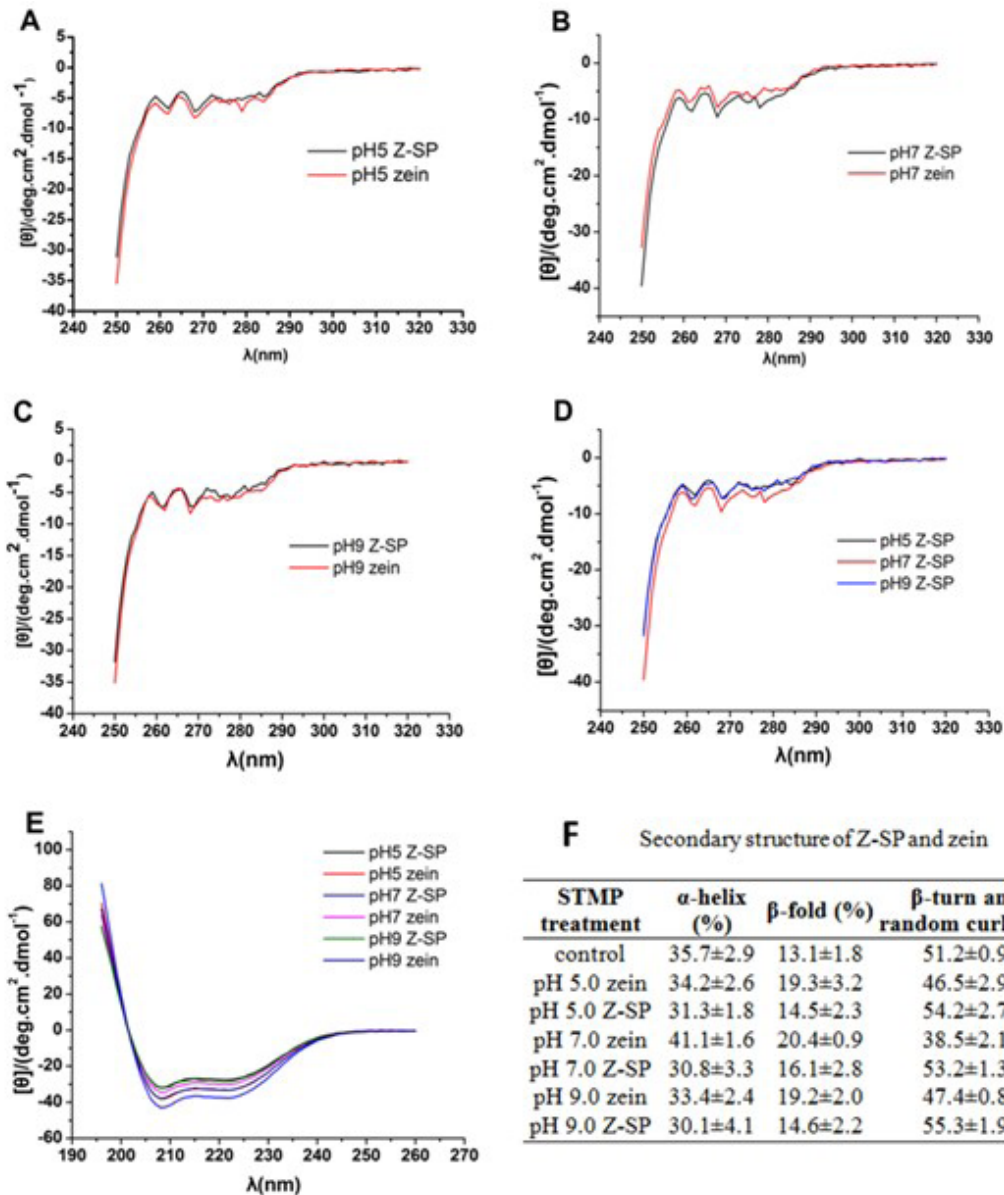

STMP treatment	α-helix (%)	β-fold (%)	β-turn and random curl (%)
control	35.7±2.9	13.1±1.8	51.2±0.9
pH 5.0 zein	34.2±2.6	19.3±3.2	46.5±2.9
pH 5.0 Z-SP	31.3±1.8	14.5±2.3	54.2±2.7
pH 7.0 zein	41.1±1.6	20.4±0.9	38.5±2.1
pH 7.0 Z-SP	30.8±3.3	16.1±2.8	53.2±1.3
pH 9.0 zein	33.4±2.4	19.2±2.0	47.4±0.8
pH 9.0 Z-SP	30.1±4.1	14.6±2.2	55.3±1.9

Figure 3. CD spectra of Z-SP and zein (A, B, C and D are near ultraviolet CD spectra of Z-SP and zein at different pH; E is far ultraviolet CD spectra of Z-SP and zein; F is secondary structure of Z-SP and zein).

3.5 FT-IR analysis

FT-IR can be used to detect the structural changes of proteins (Liu et al., 2022). The FT-IR absorbance spectra of zein, Z-SP and STMP are exhibited in Figure 4. STMP had the larger characteristic peaks at 1296 and 1102 cm^{-1} for P=O. However, these peaks did not appear in the FT-IR spectrum of Z-SP. Similarly, the characteristic peaks of STMP at 985 and 774 cm^{-1} (for P-O-P) were not found. It could be concluded that zein and STMP formed a complex. In Figure 4A, the amide I band of zein located at 1645.34 cm^{-1}. After STMP modification, the amide I band had a significant blueshift (from 1645.34 to 1645.76 cm^{-1}) (Figure 4B), which might be related to the stretching vibration of C=O or the bending vibration of N-H. The N-H bending vibration at 1554 cm^{-1} and the C-H angular vibration at 1414 cm^{-1} also resulted in a redshift (from 1554.47 to 1554.11 cm^{-1}) and blueshift (from 1414.47 to 1414.93 cm^{-1}), respectively. a weak peak appearing at 1165 cm^{-1} was also observed, which might be the plane bending vibration of NH$_2$ in glutamine (Gillgren et al., 2009). After STMP modification, the peak had a significant redshift from 1165.52 to 1161.96 cm^{-1}. It could be speculated that STMP might combine with the NH$_2$ group of glutamine in zein, thus causing plane bending vibration of the group. The structure changes of zein caused by STMP modification are helpful to improve the membrane forming ability.
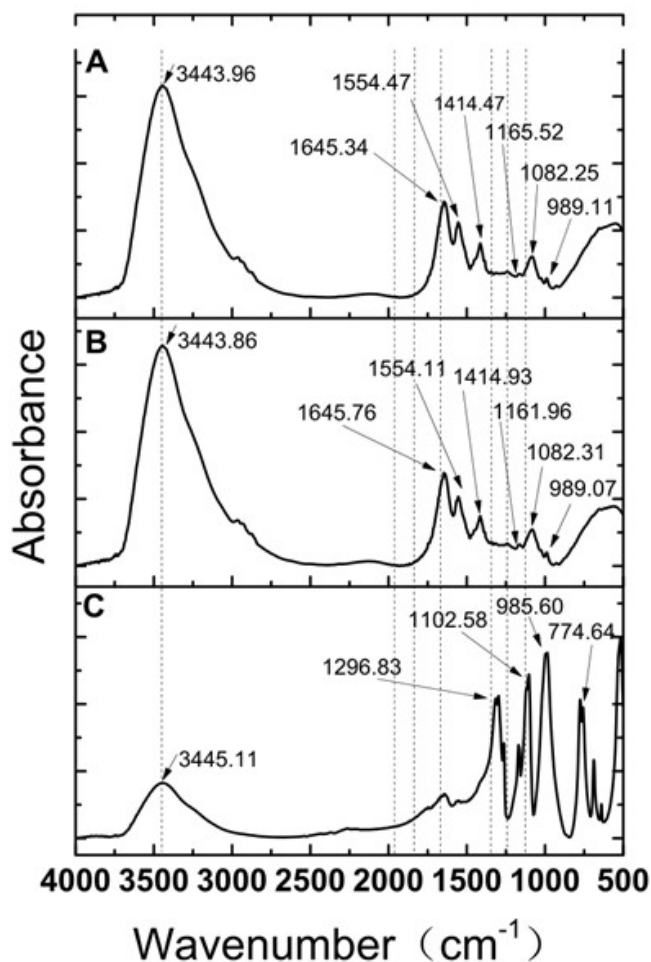
Figure 4. FTIR spectra of zein (A), Z-SP (B) and STMP (C).

4 Conclusion

In this study, STMP was used as a cross-linking agent to modify zein. Response surface methodology was used to optimize the modification process. The optimal modification conditions were as follows: R$_{S/Z}$ 0.03, pH 6.8, reaction time 2 h, reaction temperature 25 °C. The viscosity of modified zein increased with the increasing shear rate, which was attributed to the structural changes according to circular dichroism (CD) and Fourier transform infrared (FTIR) analysis. Our results can promote the development and application of zein in foods.

Conflict of interest

The authors declare no conflict of interest.

Acknowledgements

References

Bozdogan, N., Ormanli, E., Kumcuoglu, S., & Tavman, S. (2022). Pear pomace powder added quinoa-based gluten-free cake formulations: effect on pasting properties, rheology, and product quality. *Food Science and Technology*, 42, e39121. http://dx.doi.org/10.1590/fst.39121.

Byler, D. M., & Susi, H. (1986). Examination of the secondary structure of proteins by deconvolved FTIR spectra. *Biopolymers*, 25(3), 469-487. http://dx.doi.org/10.1002/bip.360250307. PMid:3697478.

Cazón, P., Velazquez, G., Ramírez, J. A., & Vázquez, M. (2017). Polysaccharide-based films and coatings for food packaging: a review. *Food Hydrocolloids*, 68, 136-148. http://dx.doi.org/10.1016/j.foodhyd.2016.09.009.

Forato, L. A., Bicudo, T. D. C., & Colnago, L. A. (2003). Conformation of α zeins in solid state by Fourier transform IR. *Biopolymers*, 72(6), 421-426. http://dx.doi.org/10.1002/bip.10481. PMid:14587064.

Geng, S., Li, Y., Lv, J., Ma, H., Liang, G., & Liu, B. (2022). Fabrication of food-grade Pickering high internal phase emulsions (HIPEs) stabilized by a dihydromyricetin and lysozyme mixture. *Food Chemistry*, 373(Pt B), 131576. http://dx.doi.org/10.1016/j.foodchem.2021.131576. PMid:34799133.

Gillgren, T., Barker, S. A., Belton, P. S., Georget, D. M. R., & Stading, M. (2009). Plasticization of zein: a thermomechanical, FTIR, and dielectric study. *Biomacromolecules*, 10(5), 1135-1139. http://dx.doi.org/10.1021/bm801374q. PMid:19317398.

Gouin, H. (2003). The wetting problem of fluids on solid surfaces. Part 2: the contact angle hysteresis. *Continuum Mechanics and Thermodynamics*, 15(6), 597-611. http://dx.doi.org/10.1007/s00161-003-0137-1.

Greenfield, N. J. (2006). Using circular dichroism spectra to estimate protein secondary structure. *Nature Protocols*, 1(6), 2876-2890. http://dx.doi.org/10.1038/nprot.2006.202. PMid:17406547.

Kasaai, M. R. (2018). Zein and zein -based nano-materials for food and nutrition applications: a review. *Trends in Food Science & Technology*, 79, 184-197. http://dx.doi.org/10.1016/j.tifs.2018.07.015.

Kaya, S., & Boccaccini, A. R. (2017). Electrophoretic deposition of zein coatings. *Journal of Coatings Technology and Research*, 14(3), 683-689. http://dx.doi.org/10.1007/s11998-016-9885-2.

Khalil, A. A., Deraz, S. F., Elrahman, S. A., & El-Fawal, G. (2015). Enhancement of mechanical properties, microstructure, and

antimicrobial activities of zein films cross-linked using succinic anhydride, eugenol, and citric acid. *Preparative Biochemistry & Biotechnology*, 45(6), 551-567. http://dx.doi.org/10.1080/10826068.2014.940967. PMid:25036665.

Li, J., Geng, S., Zhen, S., Lv, X., & Liu, B. (2022). Fabrication and characterization of oil-in-water emulsions stabilized by whey protein isolate/phloridzin/sodium alginate ternary complex. *Food Hydrocolloids*, 129, 107625. http://dx.doi.org/10.1016/j.foodhyd.2022.107625.

Liu, X., Geng, S., He, C., Sun, J., Ma, H., & Liu, B. (2022). Preparation and characterization of a dihydromyricetin–sugar beet pectin covalent polymer. *Food Chemistry*, 376, 131952. http://dx.doi.org/10.1016/j.foodchem.2021.131952. PMid:34973639.

Nascimento, G. E., Simas-Tosin, F. F., Iacomini, M., Gorin, P. A. J., & Cordeiro, L. M. C. (2016). Rheological behavior of high methoxyl pectin from the pulp of tamarillo fruit (*Solanum betaceum*). *Carbohydrate Polymers*, 139, 125-130. http://dx.doi.org/10.1016/j.carbpol.2015.11.067. PMid:26794955.

Qi, P. X., Ren, D. X., Xiao, Y. P., & Tomasula, P. M. (2015). Effect of homogenization and pasteurization on the structure and stability of whey protein in milk. *Journal of Dairy Science*, 98(5), 2884-2897. http://dx.doi.org/10.3168/jds.2014-8920. PMid:25704975.

Song, X. Y., & Wang, Y. Q. (2021). Development and characterization of edible bilayer films based on iron yam-pea starch blend and corn zein. *Food Science and Technology*, 41(Suppl. 2), 684-694. http://dx.doi.org/10.1590/fst.29820.

Wang, P., Sheng, F., Tang, S. W., ud-Din, Z., Chen, L., Nawaz, A., Hu, C., & Xiong, H. (2018). Synthesis and characterization of corn starch crosslinked with oxidized sucrose. *Stärke*, 71(5-6), 1800152. http://dx.doi.org/10.1002/star.201800152.

Yan, Y. Y., Wang, Q., Sun, L. H., & Zhang, X. F. (2022). Extraction, preparation, and carboxymethyl of polysaccharide from *Lotus* root. *Food Science and Technology*, 42, e17822. http://dx.doi.org/10.1590/fst.17822.

Yao, Y., Shi, Y., An, P., Zhang, R., Wang, Z., Hu, X., & Wan, Y. (2022). Optimization of preparation of calcium propionate from eggshell by Response Surface Methodology (RSM). *Food Science and Technology*, 42, e25322. http://dx.doi.org/10.1590/fst.25322.

Yıldırım-Yalçın, M., Şeker, M., & Sadıkoğlu, H. (2019). Development and characterization of edible films based on modified corn starch and grape juice. *Food Chemistry*, 292, 6-13. http://dx.doi.org/10.1016/j.foodchem.2019.04.006. PMid:31054693.

Zhang, B., Luo, Y., & Wang, Q. (2011). Effect of acid and base treatments on structural, rheological, and antioxidant properties of α-zein. *Food Chemistry*, 124(1), 210-220. http://dx.doi.org/10.1016/j.foodchem.2010.06.019.

Zhang, Y., Cui, L., Che, X., Zhang, H., Shi, N. Q., Li, C., Chen, Y., & Kong, W. (2015). Zein-based films and their usage for controlled delivery: origin, classes and current landscape. *Journal of Controlled Release*, 206, 206-219. http://dx.doi.org/10.1016/j.jconrel.2015.03.030. PMid:25828699.